

# MULTI-USER CHANNEL ESTIMATION IN OFDMA UPLINK SYSTEMS BASED ON IRREGULAR SAMPLING AND REDUCED PILOT OVERHEAD

*Peter Fertl and Gerald Matz*

Institute of Communications and Radio-Frequency Engineering, Vienna University of Technology  
Gusshausstrasse 25/389, A-1040 Vienna, Austria  
phone: +43 1 58801 38942; fax: +43 1 58801 38999; email: peter.fertl@nt.tuwien.ac.at

## ABSTRACT

This paper considers multiuser OFDMA uplink transmissions over doubly selective channels. We propose a pilot-aided channel estimator based on irregular sampling techniques. Our novel estimator features several benefits: it has low complexity, excellent performance, and enables highly flexible subcarrier allocation. Simulation results show that our scheme significantly outperforms conventional least-squares channel estimation and allows to support high-rate users with reduced pilot overhead.

**Index Terms**— OFDMA, uplink, channel estimation, irregular sampling, multiuser channels

## 1. INTRODUCTION

**Motivation.** Recently, orthogonal frequency division multiple access (OFDMA) has been recognized as a powerful multiuser communications scheme for broadband wireless systems. Multiple access is achieved via highly flexible subcarrier allocations that avoid intracell interference and, in conjunction with frequency hopping and coding, allow to exploit diversity gains and reduce intercell interference. A further advantage is the resilience to multipath propagation. OFDMA is thus a strong candidate for high speed packet transmissions in cellular environments. Current applications are WiMAX (IEEE 802.16 [1]) and 3GPP long-term evolution (LTE) [2].

Accurate channel state information (CSI) is crucial for resource allocation, adaptive modulation, and coherent detection. Channel estimation in OFDMA uplinks is challenging, however, since different channel responses for the individual users need to be tracked simultaneously at the base station. OFDMA systems with adaptive resource allocation are even more critical since the uplink channels have to be estimated over the whole frequency band (all subcarriers). Usually, pilot-aided estimation schemes are used, i.e. training data is embedded into the transmit signal. With conventional OFDM, regular pilot lattices enable efficient channel estimation via least-squares (LS) [3] or minimum mean-square error (MMSE) interpolation [4]. These techniques are difficult to use in OFDMA since discontinuous user allocations only allow for irregular (scattered) pilot patterns. To overcome this problem, current OFDMA uplink systems collect several adjacent subcarriers and time slots into subsets referred to as tiles. Channel estimation is then performed for each tile separately, which requires that each tile contains a sufficient number of pilots. As a consequence, the number of pilots increases with the number of tiles assigned to an active user, thus affecting the users net data rate. As an example, WiMAX uses  $3 \times 4$  tiles with four pilots, i.e., a pilot

overhead of  $\sim 30\%$ . There is few work dealing with the problem described above [5, 6].

**Contributions.** The main contributions of this paper can be summarized as follows:

- We propose to use an irregular sampling approach for channel estimation in OFDMA uplinks with scattered pilot symbols.
- Following this approach, we present a low-complexity iterative algorithm with automatic stopping rule that delivers accurate CSI.
- We discuss how the channel estimation error is impacted by the number and arrangement of the pilots and the maximum delay and Doppler.
- We assess the performance of our method via extensive numerical simulations of a typical OFDMA uplink system.

The main advantages of our irregular sampling based channel estimation scheme are (i) excellent performance as compared to conventional LS channel estimation; (ii) enhanced flexibility regarding user allocation, frequency hopping patterns, and pilot arrangement; (iii) the potential for reduced pilot overhead. The latter property is due to the fact that the number of pilots necessary for our scheme is determined by the users' channel conditions and *not* by the number of allocated subcarriers (tiles). We note that irregular sampling ideas have recently been independently used in a different channel estimation context in [7].

## 2. SYSTEM MODEL

**General Transmission Setup.** We consider an OFDMA uplink system with  $K$  subcarriers, total bandwidth  $B$ , and perfect user synchronization. A packet consists of  $N$  consecutive symbol periods and is shared by  $U$  (active) users. The packet is partitioned into tiles (cf. Fig. 1), i.e., contiguous time-frequency blocks of size  $N_t \times K_t$ , that represent the smallest unit that can be allocated to a user. The system granularity (i.e., the tile size) is chosen depending on the maximum number of users, channel conditions, etc.

Each user is being allocated a unique collection of tiles in a flexible manner, depending on his rate requirements. The distribution of one user's tiles may be completely irregular due to permutations [1] and frequency hopping. Each user performs channel coding, interleaving, and symbol mapping and transmits the resulting symbols within the tiles he has allocated.

**Receive Signal Model.** We assume perfect synchronization and that the channels from all users to the base station remain (approximately) constant within one OFDMA symbol. The maximum delay is suggested shorter than the cyclic prefix length. The demodulated base station receive signal is then given by

$$Y[n, k] = \sum_{u=1}^U H^{(u)}[n, k]X^{(u)}[n, k] + Z[n, k].$$

This work was supported by the STREP project MASCOT (IST-026905) within the Sixth Framework Programme of the European Commission and by the WWTF project MOHAWI (MA 44).

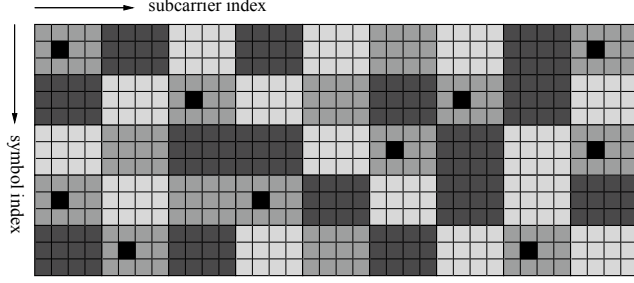


**Fig. 1.** Illustration of an OFDMA receive packet with three users (different gray shadings) and  $4 \times 3$  tiles. The pilot symbols of one user are indicated by black squares.

Here,  $u \in \{1, \dots, U\}$  denotes the user index,  $n \in \{0, \dots, N-1\}$  the symbol index, and  $k \in \{0, \dots, K-1\}$  the subcarrier index; furthermore,  $X^{(u)}[n, k]$  and  $H^{(u)}[n, k]$  are the transmit symbols and channel coefficients corresponding to user  $u$ , and  $Z[n, k]$  is additive white Gaussian noise with variance  $\sigma_z^2$ . We use the convention that  $X^{(u)}[n, k] = 0$  for  $(n, k) \notin \mathcal{U}^{(u)}$ , where  $\mathcal{U}^{(u)}$  denotes the symbol and subcarrier positions allocated to user  $u$ . Moreover, some of the transmit symbols carry a pilot rather than data. The collection of pilot positions of user  $u$  is denoted by  $\mathcal{P}^{(u)}$  and the number of pilots is  $P^{(u)} = |\mathcal{P}^{(u)}|$ . We assume that  $\mathcal{P}^{(u)}$  is contained in a subset of the tiles allocated to user  $u$ .

**Channel Model.** We assume that all user channels are doubly dispersive Rayleigh fading channels satisfying the wide-sense stationary uncorrelated scattering (WSSUS) assumption [8]. The channel coefficients  $H^{(u)}[n, k]$  are the two dimensional (2-D) Fourier transform of the spreading function  $S^{(u)}[m, l]$  ( $m, l$  denote discrete delay and Doppler) [9],

$$H^{(u)}[n, k] = \frac{1}{\sqrt{KN}} \sum_{m=0}^{M_\tau-1} \sum_{l=-M_v/2}^{M_v/2} S^{(u)}[m, l] e^{-j2\pi(\frac{mk}{K} - \frac{ln}{N})}. \quad (1)$$

Here, we assumed that  $S^{(u)}[m, l]$ ,  $u = 1, \dots, U$ , is (at least effectively) supported within the rectangle  $[0, M_\tau - 1] \times [-M_v/2, M_v/2]$  with  $M_\tau$  and  $M_v$  denoting the channels' maximum delay spread and maximum Doppler spread<sup>1</sup>, respectively. In practice,  $M_\tau \ll K$  and  $M_v \ll N$ , which implies that  $H^{(u)}[n, k]$  is a 2-D lowpass function.

### 3. PROPOSED CHANNEL ESTIMATION

**Basic Idea.** Since all users transmit over separate channels, the receiver has to estimate  $U$  different channels  $H^{(u)}[n, k]$ ,  $u = 1, \dots, U$ . At the pilot positions, the LS estimates are obtained according to  $\hat{H}_{LS}^{(u)}[n, k] = Y[n, k]/X^{(u)}[n, k]$ ,  $(n, k) \in \mathcal{P}^{(u)}$ . It follows that

$$\hat{H}_{LS}^{(u)}[n, k] = H^{(u)}[n, k] + \frac{Z[n, k]}{X^{(u)}[n, k]}, \quad (n, k) \in \mathcal{P}^{(u)}. \quad (2)$$

However, the tiles (and hence pilot positions) of a user are typically distributed in an uneven, irregular fashion (cf. Fig. 1). This prevents the use of interpolation methods for regular lattices to recover the channel coefficients  $H^{(u)}[n, k]$ ,  $[n, k] \notin \mathcal{P}^{(u)}$ . Current state of the art is to perform local channel estimation on a per-tile basis. This requires a sufficient number of pilots within each tile.

Motivated by the observation that (2) amounts to a noisy non-uniform 2-D sampling of  $H^{(u)}[n, k]$  (i.e., the sampling points do not constitute a regular lattice), we propose an alternative approach that is based on irregular sampling and reconstruction techniques (e.g. [10]). This amounts to viewing channel estimation as reconstruction

<sup>1</sup>For simplicity, we assume that  $M_v$  is even.

problem for the 2-D lowpass function  $H^{(u)}[n, k]$ . In particular, we adapt the so-called *ABC algorithm* [11, 12] to be applicable to our channel estimation problem. This algorithm was originally developed for the reconstruction of bandlimited images and is a highly efficient iterative method with excellent reconstruction performance. The abbreviation ‘‘ABC’’ signifies the central ingredients used in this 2-D reconstruction algorithm: adaptive weights (omitted in the algorithm description and in our simulations), block Toeplitz matrices, and conjugate gradient. This approach features excellent performance (see Section 5) and allows to dispose with the requirement that each tile must contain pilot symbols.

**Reconstruction Algorithm.** We next provide a more detailed mathematical description of the channel reconstruction problem and algorithm. Since the channel of each user is estimated separately, we omit the user index for simplicity in this and the next section.

Due to (1),  $H[n, k]$  can be interpreted as 2-D trigonometric polynomial of degree  $M_\tau \times (M_v + 1)$  with coefficients  $S[m, l]$ . We are given  $\hat{H}_{LS}[n_p, k_p]$ , i.e., a noisy sampled version of  $H[n, k]$ , and channel reconstruction amounts to solving the LS problem

$$\hat{H}[n, k] = \arg \min_{\hat{H}[n, k] \in \mathcal{T}} \sum_{p=1}^P |\hat{H}[n_p, k_p] - \hat{H}_{LS}[n_p, k_p]|^2, \quad (3)$$

where  $(n_p, k_p) \in \mathcal{P}$  denotes the  $P$  pilot positions and  $\mathcal{T}$  denotes the subspace of 2-D trigonometric polynomials of degree  $M_\tau \times (M_v + 1)$  characterized by (1). The cost function in (3) can be rewritten as  $(\hat{\mathbf{h}} - \hat{\mathbf{h}}_{LS})^H (\hat{\mathbf{h}} - \hat{\mathbf{h}}_{LS})$ , where  $\hat{\mathbf{h}} = [\hat{H}[n_1, k_1], \dots, \hat{H}[n_P, k_P]]^T$ ,  $\hat{\mathbf{h}}_{LS} = [\hat{H}_{LS}[n_1, k_1], \dots, \hat{H}_{LS}[n_P, k_P]]^T$ , and  $^H$  denotes (Hermitian) transposition. Furthermore, the side-constraint  $\hat{H}[n, k] \in \mathcal{T}$  is equivalent to  $\hat{\mathbf{h}} = \mathbf{V}\mathbf{s}$ , where  $\mathbf{V}$  is a  $P \times M_\tau(M_v + 1)$  double Vandermonde matrix with elements

$$V_{p,q} = \frac{1}{\sqrt{KN}} e^{-j2\pi(\frac{mk_p}{K} - \frac{ln_p}{N})}, \quad q = m + \left\lfloor \frac{M_v}{2} + l \right\rfloor M_\tau + 1;$$

moreover,  $\mathbf{s}$  is a vector of length  $M_\tau(M_v + 1)$  containing the unknown values of the spreading function  $S[m, l]$ . The optimal LS estimate of  $\mathbf{s}$  is then straightforwardly obtained as solution of

$$\mathbf{V}\hat{\mathbf{s}} = \hat{\mathbf{h}}_{LS}. \quad (4)$$

Once the LS estimate  $\hat{\mathbf{s}}$  ( $\hat{S}[m, l]$ ) has been found,  $\hat{H}[n, k]$  (defined in (3)) can be calculated according to (1). However, solving the double Vandermonde system (4) directly is inefficient and has complexity scaling with the number of pilot symbols  $P$ . To obtain a system of equations whose dimension is independent of  $P$ , frame theory suggests pre-multiplication of (4) with  $\mathbf{V}^H$  [13]. This results in the equivalent system of equations

$$\mathbf{T}\hat{\mathbf{s}} = \hat{\mathbf{s}}_{LS} \quad (5)$$

with the length- $M_\tau(M_v + 1)$  vector  $\hat{\mathbf{s}}_{LS} = \mathbf{V}^H \hat{\mathbf{h}}_{LS}$  and the  $M_\tau(M_v + 1) \times M_\tau(M_v + 1)$  matrix  $\mathbf{T} = \mathbf{V}^H \mathbf{V}$  that can be shown to be block Toeplitz with Toeplitz blocks (BTTB). However,  $\mathbf{T}$  may have large condition number (see Section 4). We thus solve (5) iteratively using the conjugate gradient (CG) method (see [14] for details), in order to achieve regularization by early termination. Moreover, the CG method shows fast convergence and is particularly well suited for efficiently solving Toeplitz-like systems.

**Computational Complexity.** It can be shown that the pre-processing (calculation of  $\mathbf{T}$  and  $\hat{\mathbf{s}}_{LS}$ ) and the post-processing (calculation of the channel estimates  $\hat{H}[n, k]$  from  $\hat{\mathbf{s}}$ ) can be implemented via 2-D fast Fourier transforms (FFTs) requiring  $O(NK \log(NK))$  operations (details can be found in [11]). Moreover, the BTTB structure of  $\mathbf{T}$  allows for an efficient implementation of the CG (see [15]). Specifically, each CG iteration involves a multiplication by  $\mathbf{T}$  that can be implemented efficiently by embedding  $\mathbf{T}$  in a block-circulant

matrix with circulant blocks and using 2-D FFTs; this requires only  $O(M_r M_v \log(M_r M_v))$  operations. Thus, the complexity of one CG iteration scales with the delay and Doppler spread but *not* with the number of pilots.

#### 4. IMPLEMENTATION DETAILS

We next deal with some aspects not covered in the general algorithm discussion of Section 3.

**Pilot Arrangement.** The convergence and performance of the CG algorithm used to solve (5) decreases with increasing condition number of  $\mathbf{T}$ . Invertibility of  $\mathbf{T}$  requires  $P \geq M_r(M_v + 1)$  and an appropriate pilot arrangement. While virtually all practical pseudo-random pilot patterns lead to invertible  $\mathbf{T}$ , the associated condition number might be poor (i.e., large), thus negatively affecting CG convergence and channel estimation error. Motivated by [12], we conjecture that the condition number  $\kappa(\mathbf{T})$  of  $\mathbf{T}$ , when augmented with adaptive weights (cf. [11]), is bounded as

$$\kappa(\mathbf{T}) \leq \frac{(K + \delta_k M_r)^2 (N + \delta_n (M_v + 1))^2}{(K - \delta_k M_r)^2 (N - \delta_n (M_v + 1))^2},$$

provided that the maximal gaps between pilots in time and frequency, denoted as  $\delta_n$  and  $\delta_k$ , are smaller than the respective Nyquist intervals  $\frac{N}{M_r+1}$  and  $\frac{K}{M_r}$ . This indicates that the condition number grows with increasing pilot spacing, maximum delay spread and maximum Doppler spread (cf. [16]). However, in our simulations we observed that the channel estimation performance degrades only gradually even if the Nyquist criterion is violated.

**Stopping Criterion.** The normalized mean-square error (MSE) of the channel estimate  $\hat{H}_r[n, k]$  obtained after  $r$  CG iterations is

$$\epsilon_r = \frac{\sum_{(n,k) \in \mathcal{U}} |\hat{H}_r[n, k] - H[n, k]|^2}{\sum_{(n,k) \in \mathcal{U}} |H[n, k]|^2} \quad (6)$$

(note that in contrast to (3), summation here is over all symbol and subcarrier positions allocated to a user). With CG based on noisy samples,  $\epsilon_r$  usually has a minimum for a certain optimum iteration number  $r_{\text{opt}}$  beyond of which it may increase (cf. [16]). In practice,  $r_{\text{opt}}$  is unknown since  $H[n, k]$  in (6) is not available. Hence, another criterion for stopping the CG iterations is required. Thus, we adapt a stopping criterion from [17] to our application, i.e., the CG iterations will be stopped as soon as

$$\|\hat{\mathbf{h}}_r - \hat{\mathbf{h}}_{\text{LS}}\|^2 \leq \gamma P, \quad \gamma = \frac{\sigma_x^2 \sigma_H^2}{\sigma_z^2}. \quad (7)$$

Here,  $\hat{\mathbf{h}}_r$  is a length- $P$  vector containing  $\hat{H}_r[n, k]$ ,  $(n, k) \in \mathcal{P}$ , and  $\sigma_x^2 = \mathcal{E}\{|X[n, k]|^2\}$  and  $\sigma_H^2 = \mathcal{E}\{|H[n, k]|^2\}$ . Note that  $\hat{\mathbf{h}}_r$ ,  $\hat{\mathbf{h}}_{\text{LS}}$ , and  $P$  in (7) are directly available and the signal-to-noise ratio (SNR)  $\gamma$  can be straightforwardly estimated.

**Delay and Doppler Spread.** The proposed channel reconstruction algorithm presupposes knowledge of the channel's maximum discrete delay spread  $M_r$  and maximum discrete Doppler spread, characterized by  $M_v$ . However, the choice of  $M_r$  and  $M_v$  is not very critical. In particular, slightly too large values do not degrade the channel estimate dramatically. The maximum delay spread equals the largest channel tap index and can usually be straightforwardly determined. A worst-case choice for  $M_r$  is provided by the length of the cyclic prefix. A reasonable rule of thumb to determine the (effective) discrete Doppler spread is given by

$$M_v = 2 \left\lfloor \frac{v_{\text{max}}}{B} (K + L_{\text{CP}}) N \right\rfloor. \quad (8)$$

Here,  $L_{\text{CP}}$  is the cyclic prefix length in samples and  $v_{\text{max}}$  is the maximum Doppler frequency in Hertz. Using the maximum terminal velocity  $\omega_{\text{max}}$ , the latter can be calculated as  $v_{\text{max}} = f_c \omega_{\text{max}} / c_0$  ( $f_c$  denotes carrier frequency and  $c_0$  is the speed of light).

#### 5. SIMULATION RESULTS

We simulated a coded OFDMA uplink system with 512 subcarriers (of which 80 serve as guard and DC carriers), bandwidth  $B = 5$  MHz, and carrier frequency  $f_c = 2$  GHz. The cyclic prefix length was  $L_{\text{CP}} = 64$  samples and the packet length was  $N = 30$  OFDMA symbols divided into 10 slots of length 3. Each slot was further split into tiles comprising 4 subcarriers. The allocation of the  $3 \times 4$  tiles to the users was performed according to [1]. Each tile contained either one (fixed-location) or no pilot symbol (cf. Fig. 1) such that there are  $3P^{(u)}/N$  pilots per slot for user  $u$ . Each user employed 16-QAM, a rate-1/2 convolutional code, and a block interleaver of appropriate size. For all users, Rayleigh fading WSSUS channels with uniform delay and Doppler profiles were simulated according to [18]. Note that these channels may vary even within an individual OFDM symbol. Throughout, a terminal velocity of  $\omega_{\text{max}} = 100$  km/h was chosen, which corresponds to  $M_v = 2$  (cf. (8)). The receiver performed zero-forcing equalization using the estimated channel and channel decoding. All results were obtained by averaging over at least 5400 OFDMA packets. As a reference method we considered conventional LS estimation which uses the channel coefficients at the pilot positions according to (2) within the whole tile.

**BER/MSE versus SNR.** We first consider  $U = 9$  users, each allocated  $P = 120$  tiles with one pilot symbol each. The maximum delay spread is  $1.4 \mu\text{s}$  corresponding to  $M_r = 7$ . Fig. 2(a) compares the BER (top) and MSE (bottom) obtained with the proposed channel estimator and with the conventional LS reference scheme (labeled 'reference') for one of the 9 users. It is seen that our scheme significantly outperforms the reference method in terms of MSE and BER; furthermore, the BER performance is almost identical to the case of perfect CSI (labeled 'ideal'). In contrast, the performance of the reference estimator saturates at high SNR since it is unable to track the channel variations within a tile. Fig. 2(a) also shows the results obtained with our method when a high-rate user is allocated twice ('2x') or four times ('4x') as much tiles while the number of pilots remains fixed (i.e., only one half or one fourth of the tiles contain a pilot). It is seen that this has almost no impact on performance, hence supporting our claim that the proposed channel estimation scheme allows to significantly reduce the pilot overhead.

**BER/MSE versus Delay Spread.** We next analyze the impact of the delay spread on the performance of our scheme at a SNR of 20 dB (the impact of the Doppler spread is analogous). We considered a setup with 18 users, each allocated  $P^{(u)} = 60$  pilots in 60 tiles, and a second one with  $U = 6$  users and  $P^{(u)} = 180$  pilots/tiles. In the first setup the pilots are much less dense, i.e., the gaps between pilot positions tend to be 3 times larger on average. Fig. 2(b) shows that our method outperforms the reference scheme and has an MSE advantage that increases with increasing number of pilots. Larger delay spreads are seen to increase the MSE of both schemes, which eventually also degrades BER performance (i.e., the delay diversity gains seen with the ideal receiver cannot be fully exploited). However, the BER degradation is only gradually (in particular for the case  $P^{(u)} = 180$ ) even though the Nyquist criterion might be violated.

**Convergence.** We finally illustrate the convergence behavior of our ABC-type channel estimator. Fig. 2(c) shows the average number of CG iterations (i.e., until the stopping criterion is satisfied) versus SNR (top) and delay spread (bottom). Parameters were chosen according to the simulations in Fig 2(a) and (b), respectively. It is seen that the number of iterations increases significantly with SNR. This can be attributed to the fact that in the low-noise regime the stopping criterion is too conservative even though estimation ac-

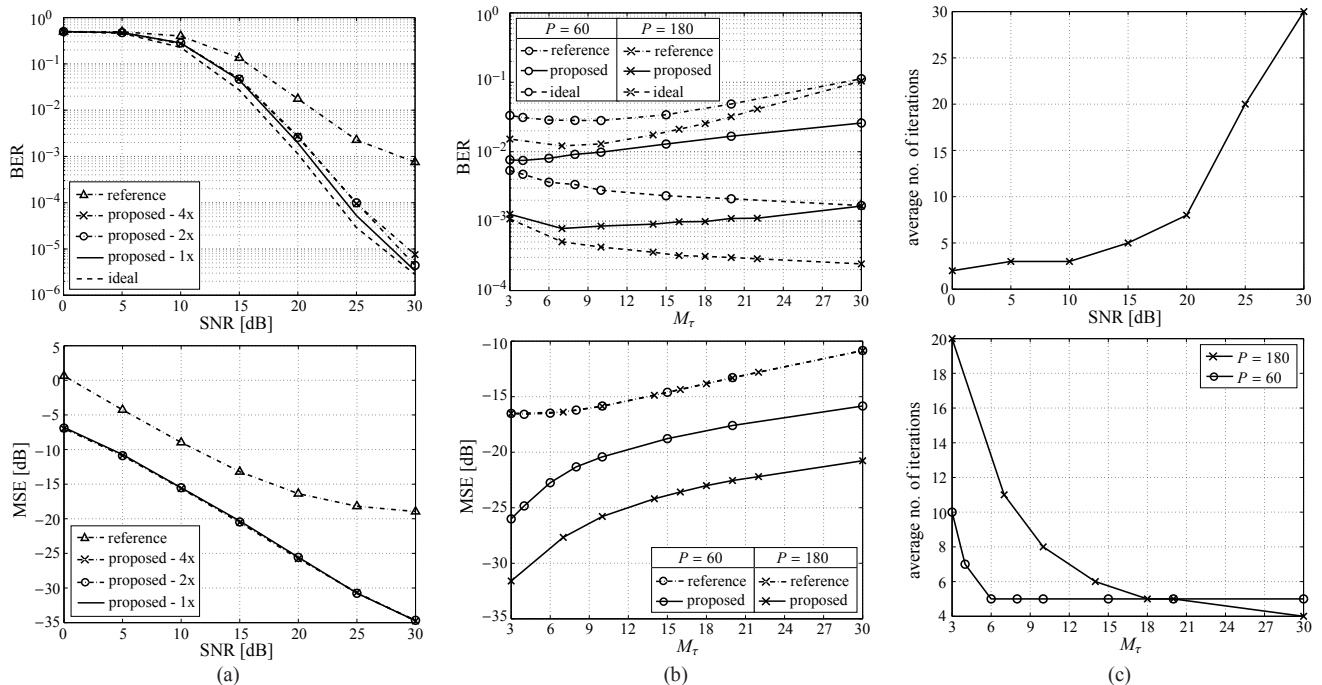


**Fig. 2.** Performance comparison of proposed method with reference scheme and with perfect CSI: (a) BER/MSE versus SNR using  $P = 120$  pilots, and (b) BER/MSE versus  $M_\tau$  for  $P = 60$  pilots and  $P = 180$  pilots; (c) Convergence over SNR and maximum delay spread.

curacy is already sufficient. In contrast, the number of iterations decreases with increasing delay spread since channels with large delay spread incur a larger MSE which can be quickly approached via the CG iterations. As a general conclusion, more iterations are required in cases where the estimation error can be made small (i.e., high SNR, low delay spread, many pilots).

## 6. CONCLUSIONS

We introduced a novel channel estimation scheme for OFDMA uplink packet transmissions over time-varying multipath channels. The proposed method uses irregular sampling techniques in order to allow flexible resource allocation and pilot arrangement. The resulting algorithm can be implemented with low complexity using CG iterations and FFTs. Simulation results show that our method outperforms conventional LS channel estimation and allows for a low pilot overhead.

## 7. ACKNOWLEDGMENTS

The authors thank T. Strohmer for providing his Matlab implementations and H. G. Feichtinger for useful discussions.

## 8. REFERENCES

- [1] IEEE LAN/MAN Standards Committee, "IEEE 802.16e: Air interface for fixed and mobile broadband wireless access systems," 2005.
- [2] 3GPP TR 25.913 (V7.3.0), *Requirements for Evolved UTRA (E-UTRA) and Evolved UTRAN (E-UTRAN)*, Mar. 2006.
- [3] E. G. Larsson, G. Liu, J. Li, and G. B. Giannakis, "Joint symbol timing and channel estimation for OFDM based WLANs," *IEEE Comm. Letters*, vol. 5, no. 8, pp. 325–327, Aug. 2001.
- [4] O. Edfors, M. Sandell, J.-J. van de Beek, S. K. Wilson, and P. O. Börjesson, "OFDM channel estimation by singular value decomposition," *IEEE Trans. Comm.*, vol. 46, no. 7, pp. 931–939, July 1998.
- [5] M. Sternad and D. Aronsson, "Channel estimation and prediction for adaptive OFDMA/TDMA uplinks, based on overlapping pilots," in *Proc. IEEE ICASSP-2005*, March 2005, vol. 3, pp. 861–864.
- [6] Y. H. Kim, K. S. Kim, and J. Y. Ahn, "Iterative estimation and decoding for an LDPC-coded OFDMA system in uplink environments," *Proc. IEEE ICC-2004*, vol. 4, pp. 2478–2482, June 2004.
- [7] O. Ureten and N. Serinken, "Decision directed iterative equalization of OFDM symbols using non-uniform interpolation," in *Proc. IEEE VTC-2006*, Montreal, Canada, Sept. 2006, to appear.
- [8] J. G. Proakis, *Digital Communications*, McGraw-Hill, New York, 3rd edition, 1995.
- [9] P. A. Bello, "Characterization of randomly time-variant linear channels," *IEEE Trans. Comm. Syst.*, vol. 11, pp. 360–393, 1963.
- [10] F. Marvasti, Ed., *Nonuniform Sampling: Theory and practice*, Kluwer Acad./Plenum Publ., New York, NY, 2001.
- [11] T. Strohmer, "Computationally attractive reconstruction of band-limited images from irregular samples," *IEEE Trans. Image Processing*, vol. 6, no. 4, pp. 540–548, 1997.
- [12] K. Gröchenig and T. Strohmer, "Numerical and theoretical aspects of non-uniform sampling of band-limited images," in *Nonuniform Sampling: Theory*, F. Marvasti, Ed., chapter 6, pp. 283 – 324. Kluwer, 2001.
- [13] R. J. Duffin and A. C. Schaeffer, "A class of nonharmonic Fourier series," *Trans. Amer. Math. Soc.*, vol. 72, pp. 341–366, 1952.
- [14] G. H. Golub and C. F. Van Loan, *Matrix Computations*, Johns Hopkins University Press, Baltimore, 3rd edition, 1996.
- [15] G. Strang, "A proposal for Toeplitz matrix calculations," *Stud. Appl. Math.*, vol. 74, pp. 171–176, 1986.
- [16] P. Fertl and G. Matz, "Efficient OFDM channel estimation in mobile environments based on irregular sampling," in *Proc. Asilomar Conf. Signals, Systems, Computers*, Pacific Grove, CA, Okt.-Nov. 2006.
- [17] M. Hanke, "Regularizing properties of a truncated Newton-CG algorithm for nonlinear inverse problems," *Numer. Funct. Anal. Optim.*, vol. 18, no. 9-10, pp. 971–993, 1997.
- [18] D. Schafhuber, G. Matz, and F. Hlawatsch, "Simulation of wideband mobile radio channels using subsampled ARMA models and multistage interpolation," in *Proc. 11th IEEE Workshop on Statistical Signal Processing*, Singapore, Aug. 2001, pp. 571–574.